Molecular Catalysis 504 (2021) 111498

Contents lists available at ScienceDirect

Molecular Catalysis

journal homepage: www.journals.elsevier.com/molecular-catalysis

Ce promoted lanthana-zirconia supported Ni catalyst system: A ternary redox system for hydrogen production

Jyoti Khatri [a], Ahmed S. Al-Fatesh [b,*], Anis H. Fakeeha [b], Ahmed A. Ibrahim [b], Ahmed E. Abasaeed [b], Samsudeen O. Kasim [b], Ahmed I. Osman [c], Rutu Patel [a], Rawesh Kumar [a,*]

[a] Department of Chemistry, Sankalchand Patel University, Visnagar, Gujarat, 384315, India
[b] Chemical Engineering Department, College of Engineering, King Saud University, P.O. Box 800, Riyadh, 11421, Saudi Arabia
[c] School of Chemistry and Chemical Engineering, Queen's University Belfast, Belfast, BT9 5AG, Northern Ireland, UK

ARTICLE INFO

Keywords:
Ceria promotion
DRM
La_2O_3-ZrO_2 supported Ni
H_2-production
Temperature programmed cyclic experiments

ABSTRACT

Hydrogen production from dry reforming of methane (DRM) over chief Ni-based catalyst is cutting edge research area due to environmental consciousness about reducing global warming gases (CH_4 and CO_2) and greener route of synthesis. Herein, ceria promoted lanthanum-zirconia supported Ni catalyst system (5NixCe/LaZr; x = 0, 1, 1.5, 2, 2.5, 3, 5 wt.%) is prepared by the wet impregnation method. It is further characterized using X-ray diffraction, infrared spectroscopy, ultraviolet spectroscopy, temperature-programmed and cyclic temperature-programmed experiments. 2.5 wt.% ceria promoted lanthana-zirconia supported Ni catalyst (5Ni2.5Ce/LaZr) has thermally stabilized the support, wide Ni-LaZr interface for CH_4 decomposition, wide basic surfaces (La_2O_3-ZrO_2) for CO_2 interaction, CO_2 coordinated La^{+3} sites (as $La_2O_2CO_3$ species), low band gap and oxygen vacancy carrying mobile oxygen (which is replenished by CO_2). Altogether, it produces more than 87 % hydrogen yield. This thorough study and fine correlation will help design industrially suitable catalyst for hydrogen production through DRM.

1. Introduction

Hydrogen is a clean and green source of energy. It is produced from biomass pyrolysis, biomass gasification [1], ethanol [2], glycerol [3], glucose [4], starch and catechol [5] through either stream or thermal reforming. Albeit, hydrogen production through clean sources as methane over a heterogeneous catalyst is highly demanded due to environmental concern, atom economy and easy separation of H_2 from the product mixture. Thermal reforming of methane [6–8], steam reforming of methane [9] and dry (CO_2) reforming of methane are some popular choice for hydrogen production. Hydrogen production from dry reforming of methane (DRM) belongs to cutting edge research which opens the hope of the efficient conversion of two global warmings gas CO_2 and CH_4 together. Among heterogeneous catalysts, Pt [10], Ru [11], Rh [12] and Ni-based catalyst system was found efficient in hydrogen production. In recent year, cheap Ni-based catalyst system has drawn most of the attention in this field. However, under highly endothermic DRM reaction, Ni undergoes serious aggregation and loss its catalytic property. So, the Ni-supported system is indeed a successful catalytic route for hydrogen production.

Ni supported on SiO_2, Al_2O_3 and ZrO_2 were found promising for H_2 production through DRM. All three supports can sustain the high-temperature reaction condition for DRM. The possible activation of CO_2 at Ni/Zr interface [13] as well as inducing Ni dispersion through the anchoring effect of Zr^{4+} species [14] makes ZrO_2 support specific than SiO_2 and Al_2O_3. Apart from that, the redox behaviour of ZrO_2 makes it superior than that of irreducible SiO_2 and Al_2O_3 support. Redox behaviour enables the support to release oxygen for possible carbon deposit oxidation [12,15–17]. Further addition of modifier/promoter in zirconia supported Ni catalyst system was found to enhance the catalytic activity. A brief literature survey of promotor/modifier utilized over zirconia supported Ni catalysts is shown in Table 1.

Research activity for preparing Ni dispersed catalyst over binary metal/non-metal oxide is also noticed in tuning acid-basic property or thermal stability [33,34]. La_2O_3 also has potent redox chemistry with La_2O_3/$La_2O_2CO_3$ set [35–37]. It will be interesting to observe the effect of the strong synergy between La_2O_3-ZrO_2 if used to support the Ni dispersed system. Presence of La_2O_3 may also influence CO_2 adsorption

* Corresponding authors.
E-mail addresses: aalfatesh@ksu.edu.sa (A.S. Al-Fatesh), kr.rawesh@gmail.com (R. Kumar).

https://doi.org/10.1016/j.mcat.2021.111498
Received 25 November 2020; Received in revised form 4 February 2021; Accepted 16 February 2021
Available online 3 March 2021

Table 1
A brief literature survey of promotor/modifier over ZrO_2 supported Ni Catalysts.

Modifier/Promoter			Support	References
Period 1	–	–	–	–
Period 2	–	–	–	–
Period 3	–	Na	ZrO_2	[18]
	–	Mg	ZrO_2	[19]
	Al	Mg	ZrO_2	[20]
	Al	–	ZrO_2	[21]
	K	Mg	ZrO_2	[22]
		Ca	ZrO_2	[23]
Period-4	Fe	—	ZrO_2	[24]
	Co	—	ZrO_2	[21]
		Mg	ZrO_2	[25]
	Co, Al	—	ZrO_2	[26]
Period-5	Y	—	ZrO_2	[27]
		Mg	ZrO_2	[28]
	La	—	ZrO_2	[29]
		—	ZrO_2	[30]
Period-6	Ce	—	ZrO_2	[31]
		Mg	ZrO_2	[32]
	Sm	—	ZrO_2	[27]

(due to its basic property) [38] and Ni-support interaction [39,40] & NiO size optimization [41,42] whereas it may inhibit H_2 consumption through RWGS reaction [43,44]. Tou et al.; have prepared nickel impregnated La_2O_3-ZrO_2 via a sol-gel method for dry reforming of coke oven gas and observed great coke resistance property [44].

Further addition of a small amount of CeO_2 in the catalyst system enhances lattice oxygen mobility, which is beneficial in eliminating carbon [45]. The synergistic role of La-Ce was also claimed as guaranteed catalyst tolerance against carbon deposition as well as lattice oxygen replenishment for the oxidation reaction [46]. Overall, we can expect as good carbon resistant and high H_2 yield with ceria promoted La_2O_3-ZrO_2 supported Ni catalytic system.

It is generally accepted that H_2 production (yield) through DRM is greatly driven by dissociation of CH_4 over Ni-supported surface followed by subsequent gasification of carbon deposit by CO_2 for cleaning the surface for the next set of CH_4 decomposition reaction ($CH_4 + CO_2 \rightarrow CO + H_2$). Later gasification of carbon deposit by H_2 due to spillover effect of hydrogen on the surface ($C + 2H_2 \rightarrow CH_4$) [47] as well as reverse water gas shift (RWGS) reaction ($CO_2 + H_2 \rightarrow CO + H_2O$) affects the H_2 yield seriously. However, gasification of carbon deposit by water (as a product of RWGS) has a positive contribution in H_2 yield.

Herein, we have prepared a lanthanum-zirconia supported Ni catalyst system and is further promoted by 1–5 % ceria. This catalytic system is employed for hydrogen production through DRM. It is characterized via X-ray diffraction, Infrared spectroscopy, Ultraviolet spectroscopy, temperature-programmed reduction (TPR), temperature-programmed desorption (TPD), temperature-programmed surface reaction (TPSR), temperature-programmed hydrogenation (TPH), temperature-programmed oxidation (TPO) and cyclic temperature-programmed experiments, i.e. CH_4-TPSR, H_2TPR-CO_2TPD-H_2TPR cycle, CO_2TPD-O_2TPO cycle and TPH-O_2TPO cycle. A fine correlation is established between characterization results and catalytic activity. This study will be helpful to design industrially robust catalyst for hydrogen production through dry reforming of methane. The objective of the research is to explore the surface catalytic excellence of Ce promoted Lanthana-Zirconia supported Ni catalyst system for hydrogen production through DRM by X-ray diffraction, Infrared & Ultra-violet spectroscopy, different temperature-programmed experiments & cyclic temperature-programmed experiments.

2. Experimental

2.1. Materials

Ni $(NO_3)_2.6H_2O$ (98 %) was purchased from Riedel-De Haen AG, Seelze, Germany, Ce $(NO_3)_3.6H_2O$ was purchased Williams Ltd, Essex, England, respectively. The support, La_2O_3+ZrO_2, was obtained as a gift from Daiichi Kigenso Kagaku Kogyo Co., Ltd. Osaka – Japan.

2.2. Catalyst preparation

The catalyst was synthesized via wet impregnation method as described in our earlier work [66]. Weighted amount of Ni $(NO_3)_2.6H_2O$ equivalent to 5.0 wt. % loading of nickel was dissolved in an aqueous medium. Weighted amount of Ce $(NO_3)_3.6H_2O$ corresponding to 1.0, 1.5, 2.0, 2.5, 3.0, 5.0 wt. % loading of cerium was added to the nickel nitrate aqueous solution. Further, the support 9 wt%La_2O_3+91wt%ZrO_2 was added to the aqueous mixture under stirring at 80 °C. The slurry was dried at 120 ℃ overnight in an oven and subsequently calcined in air at 600 ℃ for 3 h. Zirconia supported Ni catalyst, 1 % ceria promoted zirconia supported Ni catalyst, lanthana-zirconia supported Ni catalyst and 1–3 % ceria promoted lanthana-zirconia supported Ni catalyst are abbreviated as 5Ni/Zr, 5Ni1Ce/Zr, 5Ni/LaZr, 5NixCe/LaZr (where; x = 1, 1.5, 2, 2.5, 3, 5).

2.3. Catalyst characterization

Catalysts are characterized by X-ray diffraction (XRD), Infra-red spectroscopy, Ultraviolet-visible spectroscopy (UV–vis), CH_4-Temperature programmed surface reaction (CH_4-TPSR), H_2-temperature-programmed reduction (H_2-TPR), CO_2-Temperature programmed desorption (CO_2-TPD), temperature-programmed hydrogenation (TPH) and O_2-Temperature programmed oxidation (O_2-TPO). The details specification of the instrument and characterization procedure are given in supporting information (S1).

2.4. Catalyst activity test

The dry reforming of methane experiments was carried over 0.1 g of Ce promoted 5%Ni/La_2O_3+ZrO_2 catalyst at 700 ℃ under 1 atm pressure in stainless steel vertical fixed tubular reactor (PID Eng. & Tech Micro Activity Reference, 9.1 mm i.d. and 30 cm long). The catalysts were positioned by the help of a ball of glass wool during activity tests. The temperature of the reactor was monitored by an axially positioned thermocouple (K-type stainless sheathed) at the center of the catalyst bed. Before the catalytic tests, reductive pretreatment of catalyst samples was carried out under the flow of hydrogen (20 mL/min) for 60 min at 600 ℃. The mixture of gases feed $CH_4/CO_2/N_2$ in the respective volumes as 6:6:2, and the volume flow rate was 70 $mL.min^{-1}$ and 42,000 $mL(h.g_{cat})^{-1}$ gas hourly space velocity was passed through the reactor. The product gas stream was analyzed by GC (GC-2014 Shimadzu) unit equipped with a thermal conductivity detector and two columns, Porapak Q and Molecular Sieve 5A. H_2 yield % and H_2/CO molar ratio are determined by the following expressions:

$$H_2\ \text{Yield\%} = \frac{\text{Mole of } H_2 \text{ in product}}{2 \text{ x mol of } CH_{4_{in}}} \times 100$$

$$\frac{H_2}{CO} = \frac{\text{Moles of } H_2 \text{ produced}}{\text{Moles of CO produced}}$$

3. Result and discussion

3.1. Catalytic activity results

The catalytic activity results in terms of H_2 yield is shown in Fig. 1. Zirconia supported Ni catalysts are efficient to produce hydrogen with a 43 % yield. After adding the ceria promoter (5Ni1Ce/Zr), a rise in H_2 yield (47 %) was noticed. However, a marked increase of H_2 yield about 80 % was only noticed if lanthana-zirconia support was used in place of only zirconia support. 5Ni/LaZr catalyst showed 80 % H_2 yield. Further

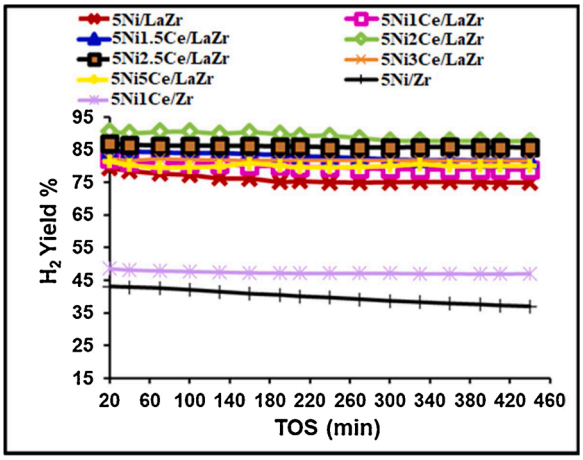

Fig. 1. Catalytic performance of 5NiyCe/Zr and 5NixCe/LaZr (x = 0, 1, 1.5, 2, 2.5, 3, 5 and y = 0, 1) in different catalytic system for dry reforming of methane (DRM).

promotional effect of ceria was also noticed up to 2.5 % Ceria addition. 5Ni1Ce/LaZr, 5Ni1.5 Ce/LaZr and 5Ni2Ce/LaZr showed 82 %, 85 % and 91 % H_2 yield, respectively. Our target was to find out a catalytic system composition that has both high and stable performance toward H_2 yield. 5Ni2.5Ce/LaZr catalyst retained 86–87 % H_2 yield up to more than 420 min. 2.5 % ceria loading was found to be the optimum loading in term of catalytic activity. Further increases in ceria loading caused a drop in H_2 yield; however, the activity of the catalysts remains stable. 5Ni3Ce/LaZr and 5Ni5Ce/LaZr showed 81–82 % and 80–81 % H_2 yield up to more than 420 min of reaction, respectively. H_2/CO ratio of all ceria promoted lanthana-zirconia supported Ni catalyst system are found close to 1 (Fig S2). Thermogravimetric analysis (TGA) analysis shows decreased carbon deposits over the catalyst surface with increasing ceria loading (Fig. S3).

3.2. Characterization results

The XRD profiles of spent catalysts of 5NixCe/Zr (x = 0, 1) are shown in (Fig. 2 (A)). Spent zirconia supported Ni (Spent 5Ni/Zr) catalyst shows monoclinic zirconium oxide phase (space group: P21/C, JCPDS no. 00-007-0343), crystalline carbon phases (space group: P63mc, JCPDS no. 01-075-1621) and cubic nickel oxide phase (space group: Fm3m, JCPDS no. 01-073-1519, 2θ = 37.32° at 111 plane, 2θ = 43.57° at 200 plane; 2θ = 62.92° at 220 plane). It indicates that zirconia support is prone to crystalline carbon deposition during the DRM reaction. Ceria promoted catalyst system is known to be coke resistance due to prompt mobile oxygen availability for coke oxidation. Ceria promoted

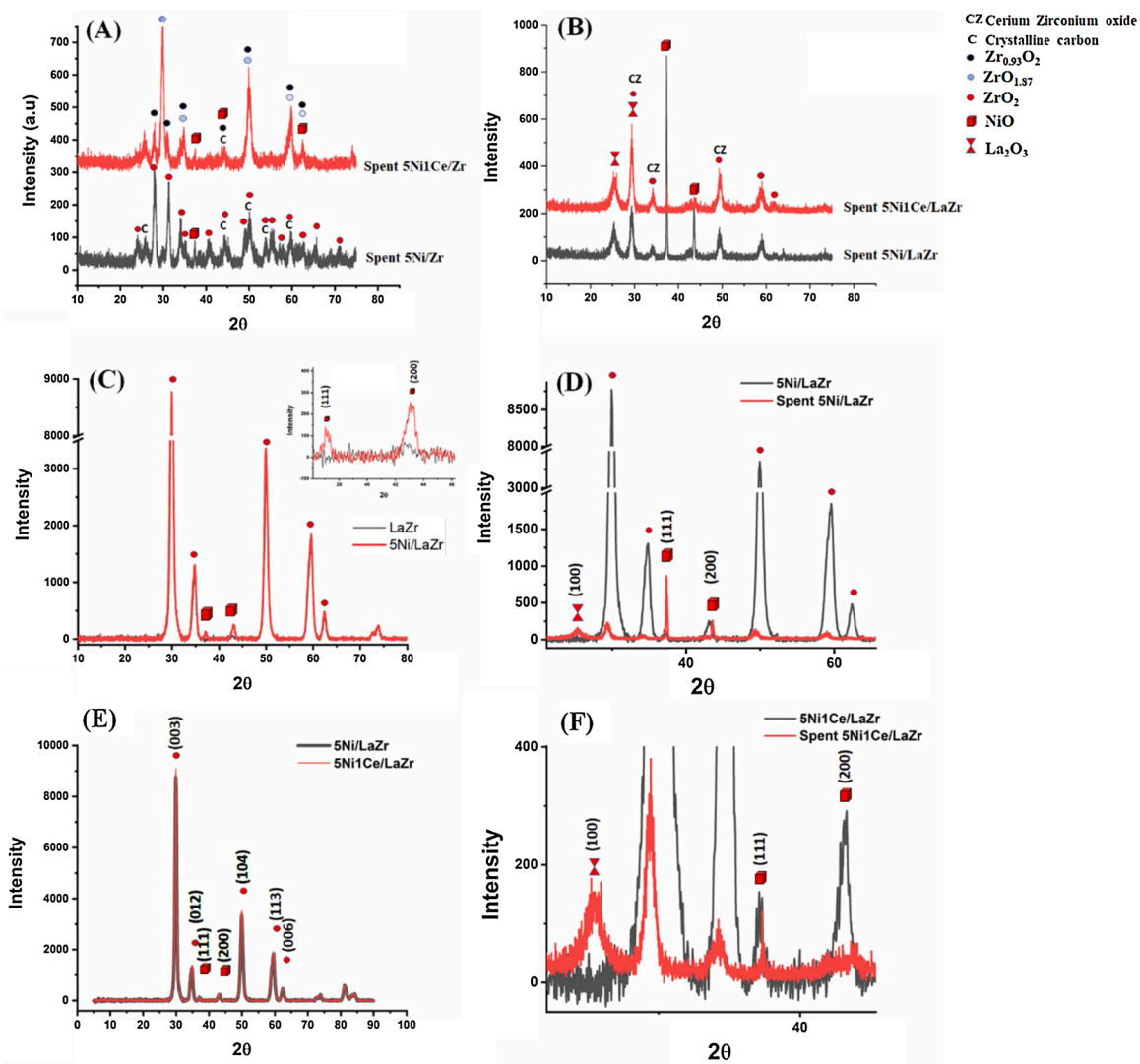

Fig. 2. XRD profile of fresh and spent 5NixCe/Zr and 5NixCe/LaZr (x = 0, 1) catalyst used for dry reforming of methane (DRM).

spent catalyst (spent 5Ni1Ce/ZrO_2) had minimum carbon phases, but it had prominent defective zirconia oxides phase as $ZrO_{1.96}$ (monoclinic Zirconium oxide, space group: P21/C, JCPDS no. 01-081-1319) and $Zr_{0.93}O_2$ (cubic Zirconium oxide, space group: Fm3m, JCPDS no. 01-081-1551). That means ceria promotional addition caused rapid wash away of crystalline carbon (by oxidation of deposit).) Overall, defective zirconia and phase transformation of zirconia phase from monoclinic to cubic zirconia at high-temperature condition limits the high catalytic performance of this catalytic system. Overall, zirconia was not a good support, and some phase stabilizer is curiously needed for higher catalytic performance.

The XRD profile of 5NixCe/LaZr (x = 0, 1) are shown in (Fig. 2(B)–(F)). After mixing lanthanum in zirconia support, no such defective phases and phase transformations were noticed (Fig. 2(B)). It indicates that lanthana stabilized the zirconia phase and now lanthana-zirconia became a good catalytic support for a high-temperature DRM reaction. However, in all spent catalyst system; hexagonal lanthanum oxide phase (Space group: P-3m1, JCPDS no. 01-083-1345; $2\theta = 25.51^\circ$ 100 plane, $2\theta = 29.37^\circ$ at 011 plane) was noticed. It indicates that the La_2O_3 phase crystallized during the high-temperature reaction. Spent 5Ni/LaZr catalyst also showed intense NiO peak at 37.32° than that without lanthana catalyst. It also an indication of poor NiO dispersion after the reaction. To resolve this issue, a small addition of ceria was found beneficial. After promotional addition of ceria in this catalyst system, spent 5Ni1Ce/LaZr showed tetragonal cerium zirconia oxide peaks (Space group: P4212, JCPDS no. 00-026-0359; $2\theta = 29.46^\circ$ at 002 plane, $2\theta = 34.31^\circ$ at 102 planes; $2\theta = 49.34^\circ$ at 212 plane) and diffused NiO crystallite peaks. It indicates that the presence of ceria or ceria-zirconia mixed oxide enhances the NiO dispersion and control the size of NiO during the high-temperature DRM reaction.

The XRD profiles lanthana-zirconia sample had zirconia oxide phases, but not the lanthanum oxide phase. It indicates that lanthanum oxide is well dispersed. After NiO addition, the cubic NiO diffraction peaks appeared at $2\theta = 37.32^\circ$ and 43.57° (Fig. 2(C)). Moreover, after the reaction; zirconium oxide diffraction peak intensity was suppressed predominantly, lanthanum oxide (01-083-1345) diffraction peak appeared, and NiO peaks about (111) intensified. After addition of ceria to "lanthana-zirconia supported Ni system", a marginal rise of zirconia oxide peaks was noticed, but no significant changes were noticed in the mean crystallite size of NiO (Fig. 2 (E) and (F)). After the reaction, the lanthanum oxide (01-083-1345) peak appeared whereas zirconium oxide as well as NiO peaks, were suppressed. It indicates that ceria does not influence NiO dispersion during catalyst preparation, but during the high-temperature DRM reaction, its presence is essential for high dispersion of NiO.

The Infra-red spectroscopy (IR) absorption bands about 3,425 and 1,625 cm^{-1} were found in all samples which are attributed to stretching and bending vibration of OH, respectively Fig. 3. Physically adsorbed CO_2 gas showed an IR absorption band at 2,349 cm^{-1} [48,49]. The IR spectra of ZrO_2 shows absorption bands at 748 and 500 cm^{-1} which are for stretching vibration of Zr-O [50–52] whereas IR spectra of La_2O_3 shows a characteristic absorption band at 3,608 cm^{-1} for stretching vibration of OH and 640 cm^{-1} for bending vibration of OH group at surface of La_2O_3 and peak at 3,450 cm^{-1} is due to La(O)OH species (Fig. 3(A)).

absorption bands at 1,464, 1,370, 1,084 and 859 cm^{-1} are attributed to $La_2O_2CO_3$ species. Among which absorption bands at 1,464 and 859 cm^{-1} are due to CO_3^{2-} symmetric stretching, vibration belongs to the pure form of typical ionic anhydrous lanthanum carbonate ($La_2(CO_3)_3$) [52,53]. The absorption band at 1370 cm^{-1} is due to "oxycarbonate strongly coordinated with La^{3+}" ($La_2O_3.CO_2$). The absorption band due to the symmetric stretch vibration of CO_3^{2-} is infrared inactive for free ion case, but in the lattice, it became active and gave an FTIR band at 1084 cm^{-1} due to change of D_{3h} symmetry of free ion to lower symmetry C_{2v} or C_s [54]. This peak was selected to estimate the proportional amount of $La_2O_2CO_3$ species because it gave only one band in the hexagonal polymorph form of $La_2O_2CO_3$ [55].

The FTIR signal of La-Zr samples shows the disappearance of the absorption band of 748 cm^{-1} for ZrO, 3608 and 640 cm^{-}—^{1} for OH group vibration at the surface of La_2O_3. It indicates that the bonding between atoms was greatly modified and isolated identity ZrO_2 and La_2O_3 were lost. The absorption band at 3450 cm^{-1} is due to La(O)OH species and was either disappeared or merged with hydroxyl peaks of zirconia/Lanthana-zirconia interface. As ZrO_2 was present in major quantity, so peaks due to vibration of OH were preserved at 3425 and 1625 cm^{-1}. Absorption bands at 1084 and 1370 cm^{-1} for "oxycarbonate strongly coordinated with La^{3+}" in $La_2O_2CO_3$ species were also found in La-Zr samples whereas peak due to anhydrous lanthanum carbonate ($La_2(CO_3)_3$) were disappeared. Small new absorption bands also appeared below 800 cm^{-1} due to La-O-La and La-O-Zr [56]. If IR spectra was taken after CO_2-TPD of 4Ni1CeLaZr sample, the absorption band of physically adsorbed CO_2 (2349 cm^{-1}) had increased, but absorption band due to surface hydroxyl (3425 and 1625 cm^{-1}) and $La_2O_2CO_3$ species (1084 and 1370 cm^{-1}) also decreased. It indicates that at high-temperature reaction condition these species were present over catalyst surface.

The FTIR signal of "ceria promoted Lanthana-Zirconia supported Ni catalyst" shows the disappearance of 1084 cm^{-1} absorption bands of $La_2O_2CO_3$ species concerning only "Lanthana-Zirconia supported Ni catalyst" Fig. 3(B). However, as ceria loading increased from 1 % to 2 %, it appeared again. It is remarkable that as ceria loading increased absorption bands of OH vibration and peaks due to $La_2O_2CO_3$, they were increasing. It indicates that ceria addition influences the surface hydroxyl as well as $La_2O_2CO_3$ population.

Pure ZrO_2 shows the UV band at 226 and 280 nm due to charge transfer from the 2p energy state of O (valence band) to 4d (x^2-y^2, z^2) energy state of Zr (conduction band) (Fig. 4(A)). It is simply represented as charge transition O^{2-} to Zr^{+4} [57,58]. Because Zr has d° configuration, so no characteristic peak for d-d transition was found. It shows a band gap of 5.14 eV (Fig. 4(B)). After the addition of 9%

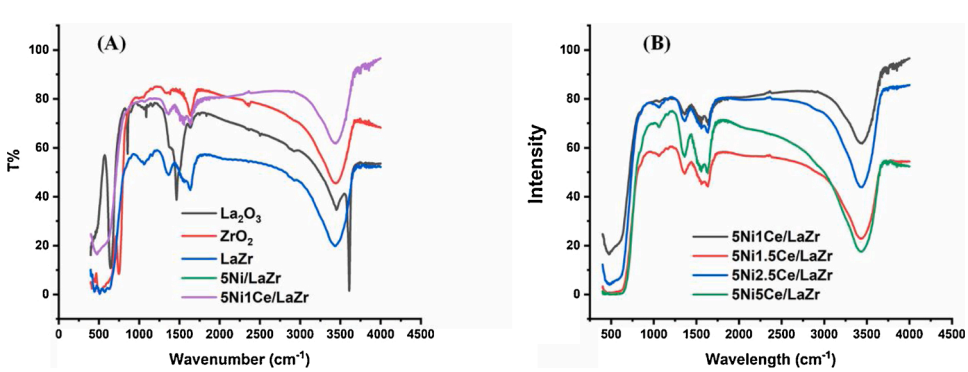

Fig. 3. IR spectra of the different catalysts used for dry reforming of methane (DRM).

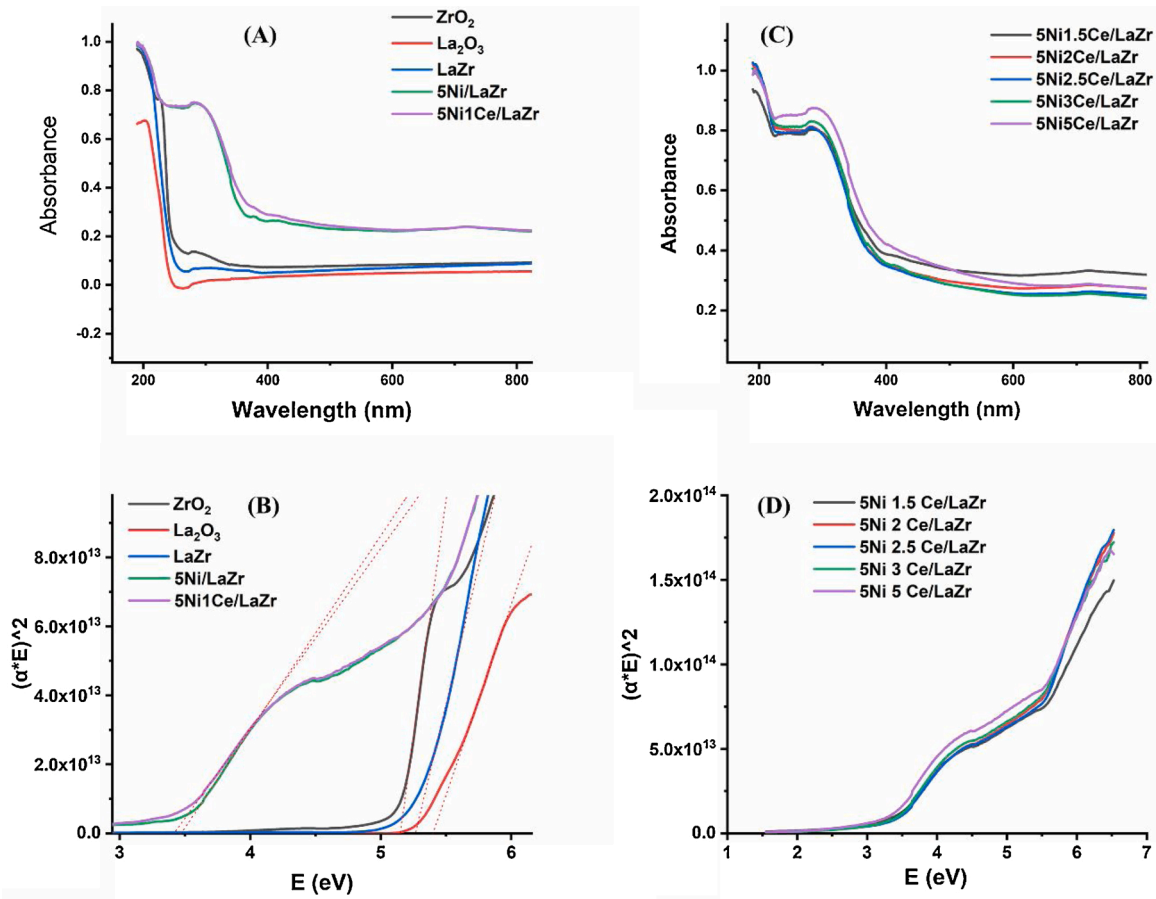

Fig. 4. Ultraviolet-visible spectroscopy (UV–vis) and band gap of the different catalyst samples.

Lanthana in Zirconia, the UV band at 226 nm was demolished completely. It indicates perturbance of charge transfer from O^{2-} to M^{+n} system. The band gap of the lanthana-zirconia system was found at 5.26 eV, which is 0.12 eV above the band gap of pure ZrO_2 (5.14 eV). It indicates that lanthana addition caused a rise of band gap, which prohibits the charge transfer from O^{2-} to M^{+n} in the new support. Thus, we can say that electronically the support lanthana-zirconia is stable than that of only zirconia.

5Ni/LaZr catalyst showed UV band at about 280 nm for the transition from O^{2-} to octahedral Ni^{+2} ($O^{2-} \rightarrow Ni^{2+}$) in NiO lattice (Fig. 4(A)) [59, 60]. The bands about 377 and 410 nm were associated with the d-d transition from $^3A_{2g}(F)$ state to $^3T_{1g}(P)$ state of Ni^{+2} in an octahedral environment, whereas band about 718 nm shows the d-d transition from $^3A_{2g}(F)$ state to $^3T_{1g}(F)$ state of the Ni^{+2} octahedral environment [58, 61–63]. This transition is more electronically favourable because the band gap of the 5Ni/LaZr catalyst system is found to reduce to 3.46 eV with respect to lanthana-zirconia system (band gap 5.14 eV) (Fig. 4(B)). After the addition of 1% ceria promoter, the band at 280 nm was intensified. It indicates that charge transfer band from O^{2-} to Ce^{+3}/Ce^{+4} merged with charge transfer band of $O^{2-} \rightarrow Ni^{2+}$ [64] As the ceria proportion was increasing, the band at 280 nm was intensified (Fig. 4 (C)). The band of d-d transition about 410 nm for $^3A_{2g}(F)$ state to $^3T_{1g}(P)$ state of Ni^{+2} (octahedral) was found to be demolished as well as ceria loading was increasing; however, the d-d transition band from $^3A_{2g}(F)$ state to $^3T_{1g}(F)$ state of Ni^{+2} (octahedra) did not be affected by ceria loading as a promoter. In all ceria loading, the band gaps of catalyst systems remained below 3.40 eV.

To study the conditions and sites of CH_4 decomposition, CH_4-temperature programmed surface reaction (CH_4-TPSR) experiment over LaZr, 5Ni/LaZr and 5Ni2.5Ce/LaZr were carried out as shown in Fig. 5.

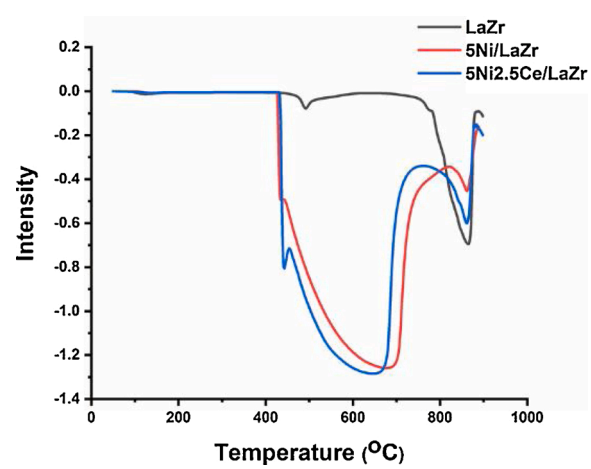

Fig. 5. CH_4-TPSR profile of catalyst used in DRM reaction.

For mesoporous lanthana-zirconia support (LaZr), a single prominent consumption peak at about 870 °C was observed due to thermal decomposition of CH_4 and promotional role of the ZrO_2 redox for oxidizing carbon species (which was formed after CH_4 thermal decomposition) [65]. At 5Ni/LaZr catalyst, a low intense low-temperature CH_4 consumption peak (~400 °C) and an intermediate temperature broad, large peak (450–800 °C) were also found. The lower temperature peak was due to CH_4 decomposition at Ni, whereas intermediate temperature peak was for CH_4 decomposition at the intimate contact between Ni and lanthana-zirconia (LaZr) interface. Promotional addition of ceria on lanthana-zirconia supported Ni catalyst did not show a significant

change in the CH_4-TSPR pattern. Overall, it indicated that the majority of CH_4 decompositions seemed to happen at Ni-LaZr interface.

To understand the reducing-oxidizing surface behaviour of 5Ni/LaZr and 5Ni2.5Ce/LaZr, we have carried out "H_2TPR-CO_2TPD-H_2TPR cycle". H_2-TPR of 5Ni/LaZr catalyst sample shows a remarkable peak in the low-temperature range (250−310 °C) and a prominent intense peak at high-temperature range (450–550 ℃) (Fig. 6 (A)). The lower peak was attributed to reduction peak of "NiO weakly interacted with the support" whereas the high-temperature peak signifies the reduction peak of "NiO strongly interacted with the support". H_2-TPR of 5Ni2.5Ce/LaZr catalyst sample showed prominent growth in lower temperature peaks than the high-temperature peak. It indicates that ceria addition promotes the cultivation of easier reducible NiO species (Fig. 6 (B)).

CO_2-TPD is carried out in continuation with H_2-TPR over 5Ni/LaZr and 5Ni2.5Ce/LaZr catalyst system. In our previous publication, the CO_2-TPD of 5Ni2.5Ce/LaZr, Samsudeen et al. [66] have reported the presence of a low concentration of weak basic sites (surface hydroxyl) at 266 ℃, intense intermediate strength basic sites (surface oxygen anion) about 400 ℃ and broad but diffuse strong basic sites (bulk oxygen anion/oxygen vacancy) about 650 ℃. As per the expectation here, when CO_2-TPD is carried out after H_2-TPR; both intermediate and high-temperature peaks disappeared. It indicates that during the reduction under H_2 stream, oxygen anion responsible for "intermediate and strong basic sites" are removed. It will be interesting to observe that may this loss be overcome by CO_2. Possibly during the CO_2-TPD, these sites may replenish oxygen from CO_2. So, in continuation of CO_2-TPD; again, H_2-TPR was carried out on the same catalyst. It gives interesting and informative results. Both peaks in low-temperature ranges, as well as high temperature, are suppressed, and an intense peak in the intermediate temperature 391 °C region appeared. Alfatish et al. claimed that the peak was due to the reduction of CeO_2-ZrO_2 and Ni—OC—e solid solutions [33]. The "H_2TPR-CO_2TPD-H_2TPR cycle" shows that 5Ni/LaZr and 5Ni2.5Ce/LaZr catalyst surface are reducible in H_2 stream, the reduced surface was re-oxidized in CO_2 stream, and then again, the oxidized surface is reducible in H_2 stream.

To understand the reactive nature of carbon deposit in reducing atmosphere, **Temperature Programmed Hydrogenation** (TPH) was carried out by 10%H_2 in Ar over spent 5Ni2.5CeLaZr, and the corresponding profile is shown in (Fig. 7(A)). A sharp peak and shoulder were found in the temperature range of 100−300 °C, whereas a broad but less intense peak was found in the region of 375–600 °C. The peak temperature position is related to the chemical equilibrium between CH_x species (x = 3, 2, 1) and their activity towards hydrogen [67,68]. Overall, these peaks are claimed due to hydrogenation of CH_x species into CH_4 by hydrogen.

O_2-Temperature Programmed Oxidation (O_2-TPO) was carried out by 10%O_2 in Ar over spent 5Ni2.5CeLaZr, and the corresponding profile is shown in (Fig. 7(B)). It shows two oxidizing peaks at 400 and 550 °C. Low temperature, the low-intensity peak is related to easily oxidizable amorphous α-carbon (intermediate of methane decomposition), whereas higher temperature, a high-intensity sharp peak is related to moderately oxidizable β-carbon species/less inert carbon species) [73, 74]. CO_2-TPD of fresh and spent 5Ni2.5CeLaZrO_2 catalyst showed that basic sites density of all types are demolished after the reaction (Fig. S4). However, if O_2-TPO is carried out after CO_2-TPD, it shows more intense peaks than simple O_2-TPO peaks. It indicates that CO_2 may react with carbon deposit and forms oxygenated species [75]. Oxygenated species are more oxidizable and give higher intensity peaks during O_2-TPO experiment [68]. So, if O_2-TPO is carried out after TPH, most intense peaks about 400 °C and 550 °C (than simple O_2-TPO peaks) are shown. In TPH, it was discussed that H_2 stream hydrogenates weakly bond carbon intermediates/species (CH_x) that desorbed as CH_4. H_2 stream may also hydrogenates strongly bond carbon intermediate/species that did not desorb during TPH but can be oxidized by oxygen during O_2-TPO experiment.

4. Discussion

CH_4 decomposition over supported Nickel is well known [76] whereas ZrO_2 system is quite basic to interact with CO_2 for a possible DRM reaction [77,78]. However, XRD profiles showed that "zirconia supported Ni catalyst" system is prone for crystalline carbon deposition during reaction which encounters inferior catalytic performance. It results in inferior catalytic H_2 yield (43 %), which slows down to 37 % after 460-minute time on stream. Ceria promotional addition to "zirconia supported Ni catalyst" causes rapid wash away of carbon (by oxidation of deposit) and so the catalytic activity increased to 47 % H_2 yield (against 43 % at zirconia supported Ni catalyst). Constant deposit wash from the catalytic active sites also causes constant yield up to 460 min time on stream. However, defective zirconia phases and fractional phase transformation of monoclinic zirconia to cubic zirconia at high temperature reaction conditions limits catalytic performance.

When support is made up of "9%lanthana-91% zirconia", infrared results show the bonding between $La_2O_3$and ZrO_2 species. The band gap of support lanthana-zirconia was increased by 0.06 eV than pure zirconia (5.08 eV). XRD profile did not show La_2O_3 related phase, but it showed phase for ZrO_2. It indicates that lanthana addition stabilizes the zirconia phase. The CO_2-TPD profile of zirconia (prepared by Silva et al. [79]) and lanthana-zirconia (prepared by Alfathesh et al. [66] are reported very similar in earlier works. After the dispersion of Ni over thermally stable lanthana-zirconia (5Ni/LaZr), defective zirconia phase was not found after the reaction. IR spectra of 5Ni/LaZr also show the presence of $La_2O_2CO_3$ species. The UV band shows a reduction of band gap to 3.12 eV (concerning 5.14 eV of lanthana-zirconia), favourable d-d transition and presence of Ni^{+2} in an octahedral environment. CH_4-TPSR shows CH_4 dissociation over Ni-support (LaZr) interface. Overall, the increasing CO_2 interaction with ZrO_2 as well as La_2O_3, prominent CH_4 decomposition at Ni-LaZr interface, excellent thermal stability, low band gap over "lanthana-zirconia supported Ni" catalyst pivots the path of DRM and ensures high H_2 yield up to 80 %. H_2 yield decreased to 75 %

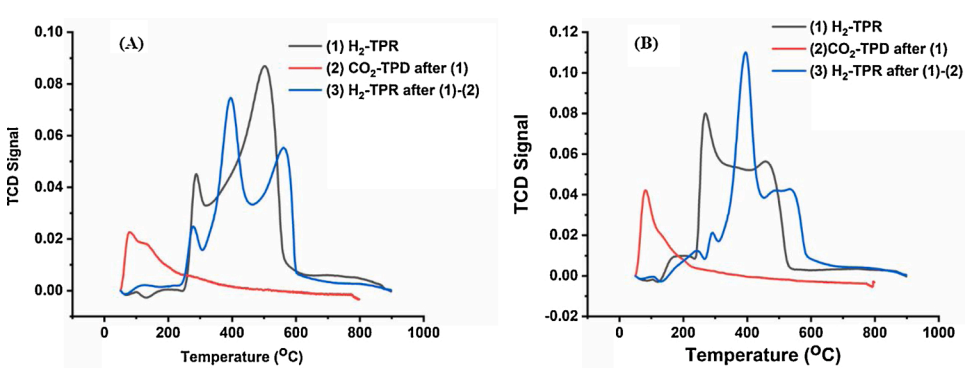

Fig. 6. (A) H_2TPR-CO_2TPD-H_2TPR cycle of 5Ni/LaZr **(B)** H_2TPR-CO_2TPD-H_2TPR cycle 5Ni/2.5CeLaZr catalyst that were used in the DRM reaction.

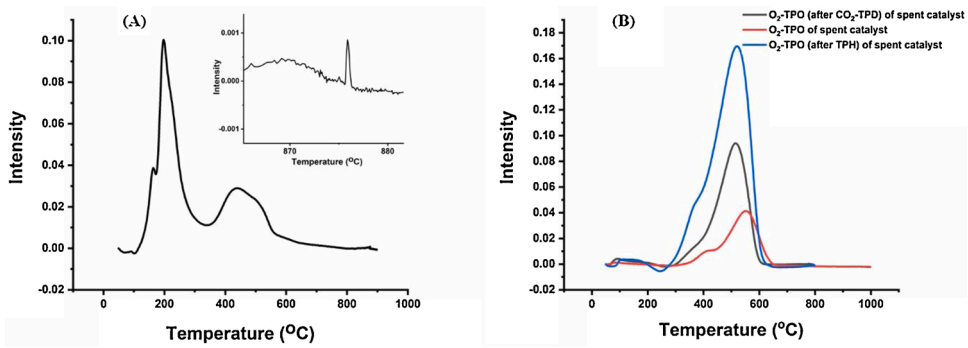

Fig. 7. **(A)** TPH profile of spent catalyst 5Ni2.5Ce/LaZr **(B)** Different O_2-TPO profile of spent catalyst 5Ni2.5Ce/LaZr.

in 460 min in time on stream test (TOS). However, the XRD profile of the spent catalyst shows the presence of high-intensity NiO. It indicates that NiO crystallites assemble during the reaction, and at the end of the reaction, NiO is poorly dispersed.

XRD profile indicates that on the promotional addition of ceria in lanthana-zirconia supported Ni catalyst (5Ni1Ce/LaZr), a ceria-zirconia mixed oxide is formed as well as NiO dispersion is maintained during the reaction. It indicates that the ceria controls the NiO dispersion during the reaction by increasing NiO-support interaction. As the loading of ceria increases, IR peak due to $La_2O_2CO_3$ gets intensified, the UV band for charge transfer transition from O^{2-} to Ce^{+3}/Ce^{+4} get intensified, and the d-d transition band for $3A_{2g}$ (F) to $3T_{1g}$ (F) in Ni^{+2} (octahedral) was demolished. It indicates that the presence of ceria, prominently influence the electronic transition over the catalyst surface where the band gap remained below 3.38 eV. At particular, ceria loading 2.5 %, Alfatish et al. has shown increased CO_2 adsorption at intermediate/strong strength basic sites or oxygen anion [66]. "H_2TPR-CO_2TPD-H_2TPR cycle" showed that CO_2 causes increased NiO-support interaction as well as oxygen replenishment form CO_2 to the catalytic surface to increase oxygen mobility for the oxidation of C-Ni_n species (which was formed after CH_4 decomposition at Ni surface). Overall, it can be said that CO_2 interaction with entire system (ZrO_2, La_2O_3, CeO_2), CH_4 decomposition over stabilized/dispersed Ni-LaZr interface, subsequent interaction of C-Ni_n species with mobile oxygen (replenished by CO_2)/Interacted CO_2 to the surface, excellent thermal stability, low band gap over 5Ni2.5Ce/LaZr catalyst governs highest H_2 yield ~87 % which remains constant throughout the 460 min in TOS. The TPH experiment shows that even ceria promoted catalyst may have some carbon deposits; however, it is reducible and removable in the early temperature range (100−300 °C) or below the reaction temperature 650 °C. As the ceria loading increases more than 2.5 %, comparable lower, but constant H_2 yield ~80 % is noticed. Ni/CeO_2 system is also a well-known catalyst for reverse water gas shift reaction (RWGS) [80]. So, possibly comparably lower H_2 yield is due to consumption of H_2 in a reverse water gas shift (RWGS) reaction ($CO_2 + H_2 \rightarrow CO + H_2O$) which is highly favoured at the high reaction temperature. "TPH followed by O_2-TPO" and "CO_2TPD followed by O_2-TPO" shows that H_2 and CO_2 environment may also induce oxygenated and hydrogenated carbon deposit at catalyst surface which may deactivate the catalyst if not removed from the catalyst surface.

Based on all characterization results, the reaction mechanism of H_2 production through DRM can be summarized in two sections. The first is the decomposition of CH_4 largely at Ni-LaZr interface into H_2 and C-Ni_n species (Reaction 1) [16]. The second is washing away of carbon deposits over Ni metal through the oxidation by CO_2. The second step should be emphasized more deeply. CO_2 may interact with basic ZrO_2 or La_2O_3-ZrO_2 surfaces, and it may be potentially adsorbed on La_2O_3 in the form of $La_2O_2CO_3$ (Reaction 2–4). At high reaction temperature, this interacted/potentially adsorbed CO_2 tends to be mobile, reaches Ni-LaZr interface, attacks carbon species (C-Ni_n) and forms two CO molecules (Reaction 5). Ceria promotional addition generates an oxygen vacancy in the catalytic system by reduction of Ce^{+4} to Ce^{+3}. It becomes new adsorption as well as decomposition sites for CO_2. Very soon, oxygen vacancies are replenished by these reactive oxygen species from the CO_2 decomposition (Reaction 6). These reactive oxygen species are mobile and vital oxidizing species for carbon species oxidation at Ni (Reaction 7). Delay in the interaction between C-Ni_n and mobile oxygen/-interacted CO_2 results in oligomer/polymer formation, leading to catalytic deactivation (Reaction 8).

$$CH_4 + Ni_n \rightarrow C\text{-}Ni_n + 2H_2 \quad (1)$$

$$ZrO_2 + CO_2 \rightarrow ZrO_2\text{——}CO_2 \quad (2)$$

$$La_2O_3 + CO_2 \rightarrow La_2O_3\text{——}CO_2 \quad (3)$$

$$La_2O_3 + CO_2 \rightarrow La_2O_2CO_3 \quad (4)$$

$$C\text{-}Ni_n + CO_2\ (\text{adsorbed}) \rightarrow 2CO + Ni_n \quad (5)$$

$$V_o + CO_2 \rightarrow CO + O;\ \text{where } V_o \text{ is oxygen vacancy} \quad (6)$$

$$C\text{-}Ni_n + O \rightarrow CO + Ni_n \quad (7)$$

$$mC\text{-}Ni_n \rightarrow C..\text{-}C..\text{-}C.. \quad (8)$$

5. Conclusion

High yield of hydrogen solely depends on the decomposition of CH_4 largely at Ni-LaZr interface into H_2 and C-Ni_n species as well as wash away of carbon deposit through oxidation by CO_2. Zirconia supported Ni catalyst is potent in H_2 production, but graphitic carbon rendered it for inferior 43 % H_2 yield. Ceria promotion also washes the carbon deposit by the mobile oxygen and amends progress in activity, but the defective support limits the H_2 yield to 47 %. The addition of 9% lanthana into zirconia support causes stabilization of zirconia phase. lanthana-zirconia supported Ni catalyst has thermally stabilized support, Ni-LaZr interface for CH_4 decomposition, wide basic surfaces CO_2 interaction, CO_2 coordinated La^{+3} sites (as $La_2O_2CO_3$ species) and low band gap. Altogether, it governs 80 % H_2 yield. Promotional addition of ceria controls the NiO dispersion during the reaction and adds mobile oxygen in the system, which is replenished back by oxygen from CO_2. 5Ni2.5Ce/LaZr shows marked 87 % H_2 yield, which remained constant up to 460 min. More than 2.5 % ceria loading shows comparably lower H_2 yield (~80 %) due to consumption of the H_2 in a reverse water-gas shift (RWGS) reaction ($CO_2 + H_2 \rightarrow CO + H_2O$).

Disclaimer

The views and opinions expressed in this paper do not necessarily reflect those of the European Commission or the Special EU Programmes Body (SEUPB).

CRediT authorship contribution statement

Jyoti Khatri: Writing - original draft, Conceptulization, Investigation. **Ahmed S. Al-Fatesh:** Supervision, Project administration, Validation, Writing - review & editing, Funding acquisition. **Anis H. Fakeeha:** Project administration, Funding acquisition, Supervision, Editing. **Ahmed A. Ibrahim:** Methodology, Formal analysis. **Ahmed E. Abasaeed:** Methodology, Formal analysis. **Samsudeen O. Kasim:** Funding acquisition, Data curation, Formal analysis. **Ahmed I. Osman:** Supervision, Editing. **Rutu Patel:** Software Formal, analysis. **Rawesh Kumar:** Funding acquisition, Supervision, Validation, Writing - review & editing.

Declaration of Competing Interest

There are no known conflicts of interest associated with this publication and this work is supported by the Deanship of Scientific Research project # No. RGP—119.

Acknowledgements

The KSU authors would like to sincerely appreciate the Deanship of Scientific Research at the King Saud University for its funding for this research group project No. (RGP-119). J K and R K acknowledge the Sankalchand Patel University for supporting research.

Appendix A. Supplementary data

Supplementary material related to this article can be found, in the online version, at doi:https://doi.org/10.1016/j.mcat.2021.111498.

References

[1] M. Ni, D.Y.C. Leung, M.K.H. Leung, K. Sumathy, An overview of hydrogen production from biomass, Fuel Process. Technol. 87 (2006) 461–472, https://doi.org/10.1016/j.fuproc.2005.11.003.

[2] G. Wu, C. Zhang, S. Li, Z. Huang, S. Yan, S. Wang, X. Ma, J. Gong, Sorption enhanced steam reforming of ethanol on Ni-CaO-Al_2O_3 multifunctional catalysts derived from hydrotalcite-like compounds, Energy Environ. Sci. 5 (2012) 8942–8949, https://doi.org/10.1039/c2ee21995f.

[3] B. Dou, B. Jiang, Y. Song, C. Zhang, C. Wang, H. Chen, B. Du, Y. Xu, Enhanced hydrogen production by sorption-enhanced steam reforming from glycerol with in-situ CO_2 removal in a fixed-bed reactor, Fuel 166 (2016) 340–346, https://doi.org/10.1016/j.fuel.2015.11.002.

[4] D. Yu, M. Aihara, M.J. Antal, Hydrogen production by steam reforming glucose in supercritical water, Energy Fuels 7 (1993) 574–577, https://doi.org/10.1021/ef00041a002.

[5] H. Schmieder, J. Abeln, N. Boukis, E. Dinjus, A. Kruse, M. Kluth, G. Petrich, E. Sadri, M. Schacht, Hydrothermal gasification of biomass and organic wastes, J. Supercrit. Fluids 17 (2000) 145–153, https://doi.org/10.1016/S0896-8446(99)00051-0.

[6] A.I. Osman, J. Meudal, F. Laffir, J. Thompson, D. Rooney, Enhanced catalytic activity of Ni on H-Al_2O_3 and ZSM-5 on addition of ceria zirconia for the partial oxidation of methane, Appl. Catal. B Environ. 212 (2017) 68–79, https://doi.org/10.1016/j.apcatb.2016.12.058.

[7] N. Gutta, V.K. Velisoju, J. Tardio, J. Patel, L. Satyanarayana, A.V.S. Sarma, V. Akula, CH_4 cracking over the Cu-Ni/Al-MCM-41 catalyst for the simultaneous production of H2 and highly ordered graphitic carbon nanofibers, Energy Fuels 33 (2019) 12656–12665, https://doi.org/10.1021/acs.energyfuels.9b02819.

[8] W. Ahmed, A.E. Awadallah, A.A. Aboul-Enein, Ni/CeO_2–Al_2O_3 catalysts for methane thermo-catalytic decomposition to COx-free H2 production, Int. J. Hydrogen Energy 41 (2016) 18484–18493, https://doi.org/10.1016/j.ijhydene.2016.08.177.

[9] A.P. Simpson, A.E. Lutz, Exergy analysis of hydrogen production via steam methane reforming, Int. J. Hydrogen Energy 32 (2007) 4811–4820, https://doi.org/10.1016/j.ijhydene.2007.08.025.

[10] S.M. Stagg-Williams, F.B. Noronha, G. Fendley, D.E. Resasco, CO_2 reforming of CH_4 over Pt/ZrO_2 catalysts promoted with La and Ce oxides, J. Catal. 194 (2000) 240–249, https://doi.org/10.1006/jcat.2000.2939.

[11] K. Nagaoka, M. Okamura, K.I. Aika, Titania supported ruthenium as a coking-resistant catalyst for high pressure dry reforming of methane, Catal. Commun. 2 (2001) 255–260, https://doi.org/10.1016/S1566-7367(01)00043-7.

[12] A.M. Efstathiou, A. Kladi, V.A. Tsipouriari, X.E. Verykios, Reforming of methane with carbon dioxide to synthesis gas over supported rhodium catalysts: II. A steady-state tracing analysis: mechanistic aspects of the carbon and oxygen reaction pathways to form CO, J. Catal. 158 (1996) 64–75, https://doi.org/10.1006/jcat.1996.0006.

[13] J.M. Wei, B.Q. Xu, J.L. Li, Z.X. Cheng, Q.M. Zhu, Highly active and stable Ni/ZrO_2 catalyst for syngas production by CO_2 reforming of methane, Appl. Catal. A Gen. 196 (2000) 0–5, https://doi.org/10.1016/S0926-860X(99)00504-9.

[14] D. Liu, X.Y. Quek, W.N.E. Cheo, R. Lau, A. Borgna, Y. Yang, MCM-41 supported nickel-based bimetallic catalysts with superior stability during carbon dioxide reforming of methane: effect of strong metal-support interaction, J. Catal. 266 (2009) 380–390, https://doi.org/10.1016/j.jcat.2009.07.004.

[15] H.Y. Wang, E. Ruckenstein, Carbon dioxide reforming of methane to synthesis gas over supported rhodium catalysts: the effect of support, Appl. Catal. A Gen. 204 (2000) 143–152, https://doi.org/10.1016/S0926-860X(00)00547-0.

[16] Z. Zhang, X.E. Verykios, S.M. Macdonald, S. Affrossman, Comparative study of carbon dioxide reforming of methane to synthesis gas over Ni/La2 O_3 and conventional nickel-based catalysts, J. Phys. Chem. 2 (1996) 744–754, https://doi.org/10.1021/jp951809e.

[17] P. Ferreira-aparicio, I. Rodr, Mechanistic aspects of the dry reforming of methane over ruthenium catalysts, Appl. Catal. A 202 (2000) 183–196, https://doi.org/10.1016/S0926-860X(00)00525-1.

[18] F. Somodi, Z. Schay, Na-promoted Ni/ZrO_2 dry reforming catalyst with high efficiency: details of Na_2O–ZrO_2–Ni interaction controlling activity and coke formation, Catal. Sci. Technol. 7 (2017) 5386–5401.

[19] J. Titus, M. Goepel, S.A. Schunk, N. Wilde, R. Gläser, The role of acid/base properties in Ni/MgO-ZrO_2–based catalysts for dry reforming of methane, Catal. Commun. 100 (2017) 76, https://doi.org/10.1016/j.catcom.2017.06.027.

[20] A.P. Tathod, N. Hayek, D. Shpasser, D.S.A. Simakov, O.M. Gazit, Mediating interaction strength between nickel and zirconia using a mixed oxide nanosheets interlayer for methane dry reforming, Appl. Catal. B Environ. 249 (2019) 106–115, https://doi.org/10.1016/j.apcatb.2019.02.040.

[21] J. Park, S. Yeo, I. Heo, T. Chang, Promotional effect of Al addition on the Co/ZrO_2 catalyst for dry reforming of CH4 authors, Appl. Catal. A Gen. 562 (2018) 120–131, https://doi.org/10.1016/j.apcata.2018.05.036.

[22] B. Mallanna, D.A. Bulushev, S. Beloshapkin, J.R.H. Ross, The effect of potassium on the activity and stability of Ni – MgO – ZrO_2 catalysts for the dry reforming of methane to give synthesis gas, Catal. Today 178 (2011) 132–136, https://doi.org/10.1016/j.cattod.2011.08.040.

[23] C. Wang, N. Sun, N. Zhao, W. Wei, J. Zhang, T. Zhao, Y. Sun, C. Sun, H. Liu, C. E. Snape, The properties of individual carbon residuals and their influence on the deactivation of Ni-CaO-ZrO_2 catalysts in CH4 dry reforming, ChemCatChem 6 (2014) 640–648, https://doi.org/10.1002/cctc.201300754.

[24] H. Lu, X. Yang, G. Gao, J. Wang, C. Han, X. Liang, C. Li, Y. Li, W. Zhang, X. Chen, Metal (Fe, Co, Ce or La) doped nickel catalyst supported on ZrO_2 modified mesoporous clays for CO and CO_2 methanation, Fuel 183 (2016) 335–344, https://doi.org/10.1016/j.fuel.2016.06.084.

[25] M. Fan, A.Z. Abdullah, S. Bhatia, Utilization of greenhouse gases through carbon dioxide reforming of methane over Ni – Co / MgO – ZrO_2: preparation, characterization and activity studies, Appl. Catal. B Environ. 100 (2010) 365–377, https://doi.org/10.1016/j.apcatb.2010.08.013.

[26] S. Mehdi, S. Mohammad, Dry reforming of greenhouse gases CH_4 / CO_2 over MgO-promoted Ni – Co / Al_2 O_3 – ZrO_2 nanocatalyst: effect of MgO addition via sol – gel method on catalytic properties and hydrogen yield, J. Solgel Sci. Technol. 70 (2014) 111–124, https://doi.org/10.1007/s10971-014-3280-1.

[27] M. Zhang, J. Zhang, Z. Zhou, S. Chen, T. Zhang, F. Song, Effects of the surface adsorbed oxygen species tuned by rare-earth metal doping on dry reforming of methane over Ni / ZrO_2 catalyst, Appl. Catal. B Environ. 264 (2020), 118522, https://doi.org/10.1016/j.apcatb.2019.118522.

[28] Y. Powders, M.J. Readey, R. Lee, J.W. Halloran, A.H. Heuep, Processing and sintering of ultrafine MgO-ZrO_2 and (MgO, Y_2O_3)-ZrO_2 powders, J. Am. Ceram. Soc. 73 (1990) 1499–1503, https://doi.org/10.1111/j.1151-2916.1990.tb09786.x.

[29] T. Yabe, K. Mitarai, K. Oshima, S. Ogo, Y. Sekine, Low-temperature dry reforming of methane to produce syngas in an electric field over La-doped Ni/ZrO_2 catalysts, Fuel Process. Technol. 158 (2017) 96–103, https://doi.org/10.1016/j.fuproc.2016.11.013.

[30] M.A. Goula, G. Siakavelas, K.N. Papageridis, N.D. Charisiou, P. Panagiotopoulou, I. V. Yentekakis, Syngas production via the biogas dry reforming reaction over Ni supported on zirconia modified with CeO_2 or La_2O_3 catalysts, WHEC 2016 - 21st World Hydrog. Energy Conf. 2016, Proc. (2016) 555–557.

[31] A. Kambolis, H. Matralis, A. Trovarelli, C. Papadopoulou, Ni / CeO_2 -ZrO_2 catalysts for the dry reforming of methane, Appl. Catal. A: Gen. 377 (2010) 16–26, https://doi.org/10.1016/j.apcata.2010.01.013.

[32] J.A. Montoya, E. Romero, A. Monzn, C. Guimon, Methane reforming with CO_2 over Ni / ZrO_2-CeO_2 and Ni / ZrO_2-MgO catalysts synthesized by sol-gel method, Stud. Surf. Sci. Catal. 4 (2000) 3669–3674.

[33] A.S. Al-fatesh, Y. Arafat, S.O. Kasim, A.A. Ibrahim, A.E. Abasaeed, A.H. Fakeeha, In situ auto-gasi fi cation of coke deposits over a novel Ni-Ce / W-Zr catalyst by sequential generation of oxygen vacancies for remarkably stable syngas production via CO_2 -reforming of methane, Appl. Catal. B Environ. 280 (2021), 119445, https://doi.org/10.1016/j.apcatb.2020.119445.

[34] A.A. Ibrahim, A.S. Al-fatesh, N.S. Kumar, A.E. Abasaeed, S.O. Kasim, A.H. Fakeeha, Dry reforming of methane using Ce-modified Ni, Catalysts 10 (2020) 242.

[35] H. Chen, H. Yu, F. Peng, H. Wang, J. Yang, M. Pan, Efficient and stable oxidative steam reforming of ethanol for hydrogen production: effect of in situ dispersion of Ir over Ir / La2 O_3, J. Catal. 269 (2010) 281–290, https://doi.org/10.1016/j.jcat.2009.11.010.

[36] M.N.N. Shafiqah, H.N. Tran, T.D. Nguyen, P.T.T. Phuong, B. Abdullah, S.S. Lam, P. Nguyen-Tri, R. Kumar, S. Nanda, D.V.N. Vo, Ethanol CO_2 reforming on La_2O_3

and CeO_2-promoted Cu/Al_2O_3 catalysts for enhanced hydrogen production, Int. J. Hydrogen Energy 45 (2020) 18398–18410, https://doi.org/10.1016/j.ijhydene.2019.10.024.
[37] S. Isarapakdeetham, P. Kim-Lohsoontorn, S. Wongsakulphasatch, W. Kiatkittipong, N. Laosiripojana, J. Gong, S. Assabumrungrat, Hydrogen production via chemical looping steam reforming of ethanol by Ni-based oxygen carriers supported on CeO_2 and La_2O_3 promoted Al_2O_3, Int. J. Hydrogen Energy 45 (2019) 1477–1491, https://doi.org/10.1016/j.ijhydene.2019.11.077.
[38] T. Hou, S. Zhang, Y. Chen, D. Wang, W. Cai, Hydrogen production from ethanol reforming: catalysts and reaction mechanism, Renew. Sustain. Energy Rev. 44 (2015) 132–148, https://doi.org/10.1016/j.rser.2014.12.023.
[39] R.M. Navarro, M.C. Álvarez-Galván, F. Rosa, J.L.G. Fierro, Hydrogen production by oxidative reforming of hexadecane over Ni and Pt catalysts supported on Ce/La-doped Al_2O_3, Appl. Catal. A Gen. 297 (2006) 60–72, https://doi.org/10.1016/j.apcata.2005.08.036.
[40] N.D. Charisiou, L. Tzounis, V. Sebastian, S.J. Hinder, M.A. Baker, K. Polychronopoulou, M.A. Goula, Investigating the correlation between deactivation and the carbon deposited on the surface of Ni/Al_2O_3 and Ni/La_2O_3-Al_2O_3 catalysts during the biogas reforming reaction, Appl. Surf. Sci. 474 (2019) 42–56, https://doi.org/10.1016/j.apsusc.2018.05.177.
[41] K.W. Siew, H.C. Lee, J. Gimbun, S.Y. Chin, M.R. Khan, Y.H. Taufiq-Yap, C. K. Cheng, Syngas production from glycerol-dry(CO_2) reforming over La-promoted Ni/Al_2O_3 catalyst, Renew. Energy 74 (2015) 441–447, https://doi.org/10.1016/j.renene.2014.08.048.
[42] W. Mo, F. Ma, Y. Ma, X. Fan, The optimization of Ni–Al_2O_3 catalyst with the addition of La_2O_3 for CO_2–CH_4 reforming to produce syngas, Int. J. Hydrogen Energy 44 (2019) 24510–24524, https://doi.org/10.1016/j.ijhydene.2019.07.204.
[43] J. Zhu, X. Peng, L. Yao, J. Shen, D. Tong, C. Hu, The promoting effect of La, Mg, Co and Zn on the activity and stability of Ni/SiO_2 catalyst for CO_2 reforming of methane, Int. J. Hydrogen Energy 36 (2011) 7094–7104, https://doi.org/10.1016/j.ijhydene.2011.02.133.
[44] W. Tao, H. Cheng, W. Yao, X. Lu, Q. Zhu, G. Li, Z. Zhou, Syngas production by CO_2 reforming of coke oven gas over Ni/La2O3-ZrO2 catalysts, Int. J. Hydrogen Energy 39 (2014) 18650–18658, https://doi.org/10.1016/j.ijhydene.2014.02.029.
[45] F. Rahbar Shamskar, F. Meshkani, M. Rezaei, Preparation and characterization of ultrasound-assisted co-precipitated nanocrystalline La-, Ce-, Zr -promoted Ni-Al_2O_3 catalysts for dry reforming reaction, J. CO_2 Util. 22 (2017) 124–134, https://doi.org/10.1016/j.jcou.2017.09.014.
[46] M. Tang, K. Liu, D.M. Roddick, M. Fan, Enhanced lattice oxygen reactivity over Fe_2O_3/Al_2O_3 redox catalyst for chemical-looping dry (CO_2) reforming of CH_4: synergistic La-Ce effect, J. Catal. 368 (2018) 38–52, https://doi.org/10.1016/j.jcat.2018.09.022.
[47] U. Chung, Effect of H_2 on formation behavior of carbon nanotubes, Bull. Korean Chem. Soc. 25 (2004) 1521–1524.
[48] A.I.D. Parkyns, The influenee of thermal pretreatment on the infrared spectrum ioxide adsorbed on alumina, Spectrum 1997 (1997) 526–531.
[49] A. Trunschke, D.L. Hoang, J. Radnik, H. Lieske, Influence of lanthana on the nature of surface chromium species in La2O3-modified CrO_x/ZrO_2 catalysts, J. Catal. 191 (2000) 456–466, https://doi.org/10.1006/jcat.1999.2791.
[50] D. Salinas, C. Sepúlveda, N. Escalona, J.L. GFierro, G. Pecchi, Sol–gel La_2O_3–ZrO_2 mixed oxide catalysts for biodiesel production, J. Energy Chem. 27 (2018) 565–572, https://doi.org/10.1016/j.jechem.2017.11.003.
[51] D. Salinas, N. Escalona, G. Pecchi, J.L.G. Fierro, Application in FAME production, Fuel 253 (2019) 400–408, https://doi.org/10.1016/j.fuel.2019.05.015.
[52] H. Sun, Y. Ding, J. Duan, Q. Zhang, Z. Wang, H. Lou, X. Zheng, Transesterification of sunflower oil to biodiesel on ZrO_2 supported La_2O_3 catalyst, Bioresour. Technol. 101 (2010) 953–958, https://doi.org/10.1016/j.biortech.2009.08.089.
[53] R.E. Przekop, P. Marciniak, B. Sztorch, A. Czapik, A. Marty, One-pot synthesis of Al_2O_3-$La_2O_2CO_3$ systems obtained from the metallic precursor by the sol-gel method, J. Non. Solids 479 (2018) 105–112, https://doi.org/10.1016/j.jnoncrysol.2017.10.020.
[54] R.P. Turcotte, L. Eyring, A.J.A. Leary, On the rare earth dioxymonocarbonates and their decomposition, Inorg. Chem. 03 (1968) 238–246, https://doi.org/10.1021/ic50072a012.
[55] T. Le Van, M. Che, J.M. Tatibouët, M. Kermarec, Infrared study of the formation and stability of $La_2O_2CO_3$ during the oxidative coupling of methane on La_2O_3, J. Catal. 142 (1993) 18–26, https://doi.org/10.1006/jcat.1993.1185.
[56] S. Wang, W. Li, S. Wang, Z. Chen, Synthesis of nanostructured $La_2Zr_2O_7$ by a non-alkoxide sol – gel method: from gel to crystalline powders, J. Eur. Ceram. Soc. 35 (2015) 105–112, https://doi.org/10.1016/j.jeurceramsoc.2014.08.032.
[57] C.V. Reddy, B. Babu, I.N. Reddy, J. Shim, Synthesis and characterization of pure tetragonal ZrO_2 nanoparticles with enhanced photocatalytic activity, Ceram. Int. 44 (2018) 6940–6948, https://doi.org/10.1016/j.ceramint.2018.01.123.
[58] Y.J.O. Asencios, J.D.A. Bellido, E.M. Assaf, Synthesis of NiO-MgO-ZrO_2 catalysts and their performance in reforming of model biogas, Appl. Catal. A Gen. 397 (2011) 138–144, https://doi.org/10.1016/j.apcata.2011.02.023.
[59] A. Fouskas, M. Kollia, A. Kambolis, C. Papadopoulou, H. Matralis, Boron-modified Ni / Al_2O_3 catalysts for reduced carbon deposition during dry reforming of methane, Appl. Catal. A Gen. 474 (2014) 125–134, https://doi.org/10.1016/j.apcata.2013.08.016.
[60] B.M.R. Damma Devaiah, Takuya Tsuzuki, Thirupathi Boningari, G. Panagiotis, Smirniotis, 5, $Ce0_{.80}M_{0.12}Sn_{0.08}O_{2-}\delta$ (M = Hf, Zr, Pr, and La) ternary oxide solid solutions with superior properties for CO oxidation, RSC Adv. (2021) 1–11, https://doi.org/10.1039/c0xx00000x, 00–00 (n.d.).
[61] P. Torres-mancera, J. Ramı, Hydrodesulfurization of 4, 6-DMDBT on NiMo and CoMo, Catal. Today 108 (2005) 551–558, https://doi.org/10.1016/j.cattod.2005.07.072.
[62] K. Hadjiivanov, M. Mihaylov, D. Klissurski, P. Stefanov, N. Abadjieva, E. Vassileva, L. Mintchev, Characterization of Ni / SiO_2 catalysts prepared by successive deposition and reduction of Ni^{2+} ions, J. Catal. 185 (1999) 314–323, https://doi.org/10.1006/jcat.1999.2521.
[63] N.f.O. Pompeo, FNichio, Study of Ni Catalysts on Different Supports to Obtain Synthesis Gas, 2005, pp. 1399–1405, https://doi.org/10.1016/j.jnoncrysol.2017.10.020.
[64] C. Mahammadunnisa, S.k. Reddy, N. Lingaiah, C.h. Subrahmanyam, $NiO/Ce_{1-x}Ni_xO_2$?d as an alternative to noble metal catalysts for CO oxidation, Catal. Sci. Technol. 3 (2013) 730–736, https://doi.org/10.1039/c2cy20641b.
[65] N. Sun, X. Wen, F. Wang, W. Peng, N. Zhao, F. Xiao, W. Wei, Y. Sun, J. Kang, Catalytic performance and characterization of Ni – CaO – ZrO_2 catalysts for dry reforming of methane, Appl. Surf. Sci. 257 (2011) 9169–9176, https://doi.org/10.1016/j.apsusc.2011.05.127.
[66] S. Olajide, A.S. Al-fatesh, A. Aidid, R. Kumar, A. Elhag, Impact of Ce-Loading on Ni-catalyst supported over La_2O_3=ZrO_2 in methane reforming with CO_2, Int. J. Hydrogen Energy (2020), https://doi.org/10.1016/j.ijhydene.2020.08.289.
[67] N.C. Triantafyllopoulos, S.G. Neophytides, The nature and binding strength of carbon adspecies formed during the equilibrium dissociative adsorption of CH_4 on Ni-YSZ cermet catalysts, J. Catal. 217 (2003) 324–333, https://doi.org/10.1016/S0021-9517(03)00062-9.
[68] N.C. Triantafyllopoulos, S.G. Neophytides, Dissociative adsorption of CH4 on NiAu/YSZ: The nature of adsorbed carbonaceous species and the inhibition of graphitic C formation, J. Catal. 239 (2006) 187–199, https://doi.org/10.1016/j.jcat.2006.01.021.
[73] D.L. Trimm, Catalysts for the control of coking during steam reforming, Catal. Today 49 (1999) 3–10, https://doi.org/10.1016/S0920-5861(98)00401-5.
[74] X. Zhang, Q. Zhang, N. Tsubaki, Y. Tan, Y. Han, Influence of zirconia phase on the performance of Ni/ZrO_2 for, Am. Chem. Soc. 1194 (2015) 135–153, https://doi.org/10.1021/bk-2015-1194.ch006.
[75] G.A.S.B. Marchon, J. Carrazza, H. Heinemann, TPD and XPS studies of O_2, CO_2, and H_2O adsorption on clean polycrystalline graphite, October, J. Hydrol. 26 (1988) 507–514, https://doi.org/10.1016/0008-6223(88)90149-2.
[76] G.A. Schouten, F.C. Kaleveld, E.W. Bootsma, Aes-leed-ellipsometry study of the kinetics of the interaction of methane with Ni(110), Surf. Sci. 63 (1977) 460–474, https://doi.org/10.1016/0039-6028(77)90359-4.
[77] Y. Wang, L. Yao, S. Wang, D. Mao, C. Hu, Low-temperature catalytic CO_2 dry reforming of methane on Ni-based catalysts: a review, Fuel Process. Technol. 169 (2018) 199–206, https://doi.org/10.1016/j.fuproc.2017.10.007.
[78] L.G. Appel, C.D. Daniela, S. Letichevsky, L.E.P. Borges, L.G. Appel, The Ni /ZrO_2 catalyst and the methanation of CO and CO_2 the Ni / ZrO_2 catalyst and the methanation of CO and CO2, Int. J. Hydrogen Energy 37 (2012) 8923–8928, https://doi.org/10.1016/j.ijhydene.2012.03.020.
[79] D.C.D. Da Silva, S. Letichevsky, L.E.P. Borges, L.G. Appel, The Ni/ZrO_2 catalyst and the methanation of CO and CO_2, Int. J. Hydrogen Energy 37 (2012) 8923–8928, https://doi.org/10.1016/j.ijhydene.2012.03.020.
[80] S. Das, J. Ashok, Z. Bian, N. Dewangan, M.H. Wai, Y. Du, A. Borgna, K. Hidajat, S. Kawi, Silica–ceria sandwiched Ni core–shell catalyst for low temperature dry reforming of biogas: coke resistance and mechanistic insights, Appl. Catal. B Environ. 230 (2018) 220–236, https://doi.org/10.1016/j.apcatb.2018.02.041.